Optics Communications 281 (2008) 4936–4939

Contents lists available at ScienceDirect

Optics Communications

journal homepage: www.elsevier.com/locate/optcom

The Yb^{3+} to Er^{3+} energy transfer in $YAl_3(BO_3)_4$ crystal

Weixiong You [a,*], Yidong Huang [b], Yujin Chen [b], Yanfu Lin [b], Zundu Luo [b]

[a] Jiangxi University of Science and Technology, Ganzhou, Jiangxi 341000, China
[b] Fujian Institute of Research on the Structure of Matter, Chinese Academy of Sciences, Fuzhou, Fujian 350002, China

ARTICLE INFO

Article history:
Received 21 April 2008
Received in revised form 10 June 2008
Accepted 18 June 2008

ABSTRACT

The Yb^{3+} to Er^{3+} energy transfer in yttrium aluminum borate (YAB) crystal is investigated with the rate equation without considering the back energy transfer. The energy transfer coefficients (W_{25}) in the crystals with different Yb^{3+} concentrations are determined and compared with those in other crystals. The transfer efficiencies and the micro-parameters of energy transfer and migration are also determined. The results show that the energy transfer from Yb^{3+} to Er^{3+} in YAB crystal is very efficient and the Yb^{3+}–Er^{3+} co-doped YAB crystal may be a good candidate for the 1.55 μm laser media.

1. Introduction

The laser emission around wavelength of 1.55 μm, which is located in the "eye-safe" region [1] and plays an important role in the optical communication as amplifier [2], can be obtained from the $^4I_{13/2} \rightarrow {}^4I_{15/2}$ transition in the Er^{3+}-doped materials. However, the Er^{3+}-doped materials cannot be efficiently pumped by the InGaAs laser diodes because of the week absorption of Er^{3+} at the wavelength of 980 nm. Generally, the solution is adding another ion as a sensitizer to improve the pumping efficiency. As a sensitizer, a broad and high absorption band around the pump wavelength is necessary. Fortunately, Yb^{3+} ion can entirely satisfy these requirements. In the Yb^{3+} and Er^{3+} co-doped materials, the pumping energy can be absorbed by Yb^{3+} efficiently and transferred to the Er^{3+}. Furthermore, the Yb^{3+} ion has only two energy levels, which makes it no excited state absorption or up-conversion losses in principle. So Er^{3+} and Yb^{3+} co-doped materials have received great attention as laser media at 1.55 μm [3–6].

$YAl_3(BO_3)_4$ (YAB) is a non-linear optical crystal with excellent chemical and physical properties [7,8], which has been demonstrated as an efficient self-frequency-doubling (SFD) material [9,10]. The structure of the crystal is trigonal with space group *R*32. The good laser results around 1.55 μm have been achieved in Yb^{3+} and Er^{3+} co-doped YAB crystal [11,12], but the energy transfer properties constitute an important factor for optimization of these crystals. So in this paper, the energy transfer from Yb^{3+} to Er^{3+} in the YAB crystal is studied on the basis of the rate equations. The energy transfer coefficient and other related parameters have been determined. The fluorescence lifetime of the $^2F_{5/2}$ level of Yb^{3+} ion has been measured and used to calculate the energy transfer efficiency. To make the analysis of energy transfer simply, the anisotropy of the crystal were not considered.

2. Experimental procedure

Yb^{3+} and Er^{3+} co-doped YAB crystals were grown by the top seeded solution method with a flux system of $NaF–MoO_3–B_2O_3$. Details of the growth procedures have been given previously [13]. The Er^{3+} concentration in the melt was fixed at 1.3 at.% whereas the Yb^{3+} concentration was varied (6, 12, 20 at.%). The real concentrations of the Yb^{3+} and Er^{3+} ions in YAB crystal were measured by inductively coupled plasma atomic emission spectrometry (ICP-AES) and summarized in Table 1. In brief, the three samples were marked with #1, #2 and #3, respectively.

The polarized absorption spectra were recorded using a spectrophotometer (Lambda900, Perkin–Elmer) in a range from 300 to 1700 nm. The resolution of the spectra is 1.0 nm. The emission cross-sections were calculated using reciprocity method [14]. The unpolarized absorption and emission cross-sections are derived from the polarized cross-sections by using $\sigma = (2\sigma^{\sigma} + \sigma^{\pi})/3$. The unpolarized emission spectra within 900–1700 nm are detected using spectrophotometer (FL920, Edinburgh) when the exciting wavelength was 657 nm corresponding to the $^4I_{15/2} \rightarrow {}^4F_{9/2}$ transition of Er^{3+} ion. The resolution of the emission spectra is 1 nm. The fluorescence decay curves at wavelength of 1030 nm were also recorded using spectrophotometer (FL920, Edinburgh) when a microsecond flash lamp (μF900, Edinburgh) was used as the pump source and the exciting wavelength was 976 nm. The signal was detected with a near-infrared (NIR) photomultiplier tube (PMT) (R5509, Hamamatsu).

3. Results and discussion

3.1. Spectroscopic properties and rate equation

Fig. 1 shows the schematic energy level diagrams of Yb^{3+} and Er^{3+} ions and the relevant transitions including the energy transfer

* Corresponding author. Fax: +86 797 8312411.
E-mail address: you_wx@126.com (W. You).

0030-4018/$ - see front matter © 2008 Elsevier B.V. All rights reserved.
doi:10.1016/j.optcom.2008.06.032

Table 1
The Yb^{3+} and Er^{3+} concentration in the melts and crystals

Samples	Melt (at.%)		Crystal (at.%)	
	Yb	Er	Yb	Er
#1	6	1.3	5.89	1.66
#2	12	1.3	12.17	1.49
#3	20	1.3	18.84	1.47

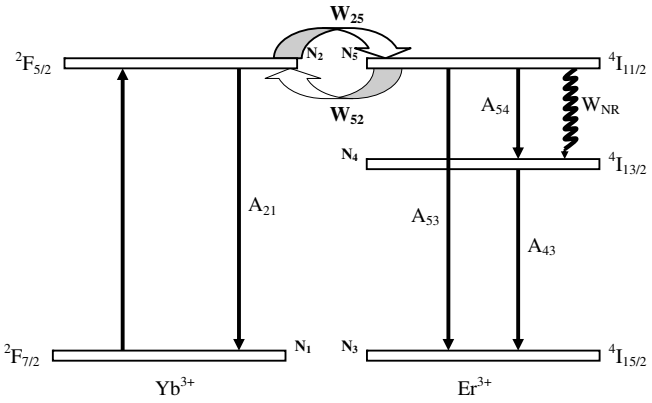

Fig. 1. The schematic energy level diagram, transitions and relevant energy transfers in the Yb, Er:YAB crystal.

processes. The energy gap between the $^2F_{7/2}$ and $^2F_{5/2}$ levels of Yb^{3+} ion (between 9613 and 10672 cm^{-1} [15]) matches well with that between the $^4I_{15/2}$ and $^4I_{11/2}$ levels of Er^{3+} ion (between 9895 and 10344 cm^{-1} [16]). Fig. 2 shows the good overlap between the normalized unpolarized absorption cross-section of Er^{3+} and emission cross-section of Yb^{3+}. It means that, when the Yb^{3+} ions are excited to the $^2F_{5/2}$ level, a resonant energy transfer from Yb^{3+} to Er^{3+} ions can occur and make the Er^{3+} ions populate the $^4I_{11/2}$ level. Then, the Er^{3+} ions in this level will decay either radiatively or non-radiatively towards lower energy levels, or through a back energy transfer to the Yb^{3+}.

Fig. 3 shows the emission spectra excited at 657 nm corresponding to the $^4I_{15/2}\rightarrow{}^4F_{9/2}$ transitions of Er^{3+} ion. It can be seen from the figure that there are many emission peaks in the range of 1480–1620 nm, which was attributed to the transitions between

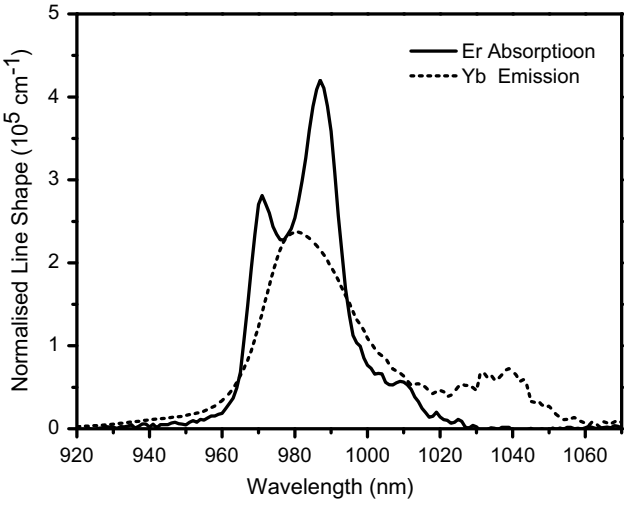

Fig. 2. Spectra overlap between the normalized emission cross-section of the Yb^{3+} sensitizer ions and the absorption cross-section of the Er^{3+} activator ions.

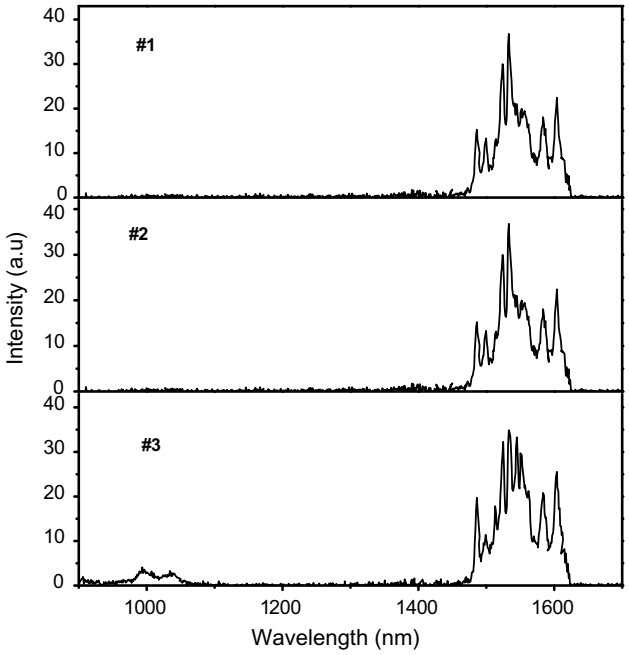

Fig. 3. The unpolarized emission spectra of Yb, Er:YAB crystal, excited at 657 nm.

the stark energy levels of $^4I_{13/2}$ and those of $^4I_{15/2}$ of the Er^{3+} ion. Furthermore, there are no emission signals or only the rather weak signals within 900–1100 nm, which means that the population in the $^4I_{11/2}$ level quickly quenched to the $^4I_{13/2}$ level due to the high phonon energy of the YAB crystal and the back energy transfer can be neglected. So in this paper the back energy transfer processes are not considered. In addition, due to the weak pump power the up-conversion is also negligible. According to the assumption above, the energy transfer dynamics can be described by the rate equations [4]

$$\frac{dN_2}{dt} = \sigma_{Yb}\Phi N_1 - N_2\left(A_{21} + W_{21}^{NR}\right) - W_{25}N_2N_3 \quad (1)$$

$$\frac{dN_4}{dt} = \left(A_{54} + W_{54}^{NR}\right)N_5 - \frac{N_4}{\tau_4} \quad (2)$$

$$\frac{dN_5}{dt} = W_{25}N_2N_3 - \frac{N_5}{\tau_5} \quad (3)$$

$$N_1 + N_2 = N_{Yb} \quad (4)$$

$$N_3 + N_4 + N_5 = N_{Er} \quad (5)$$

where N_i is the population of the i-level, A_{ij} and W_{ij}^{NR} is the radiative and non-radiative transition probabilities between the i and j level, τ_i is fluorescence lifetime of the i-level. σ_{Yb} is the Yb^{3+} absorption cross-section at the pumping wavelength, Φ is the pumping flux, N_{Er} and N_{Yb} are the concentrations of Er^{3+} and Yb^{3+} ion. W_{25} is the energy transfer coefficient from Yb^{3+} to Er^{3+}.

When the steady stat is reached, all the derivations equal to zero. Because of the weak pumping, it is assumed that, $N_1 \approx N_{Yb}$, $N_3 \approx N_{Er}$. From the equation, the results can be obtained that

$$N_2 = \frac{\sigma_{Yb}\Phi N_1\tau_2}{1 + W_{25}N_3\tau_2} \quad (6)$$

$$N_4 = (A_{54} + W_{54})N_5\tau_4 \quad (7)$$

$$N_5 = W_{25}N_2N_3\tau_5 \quad (8)$$

3.2. Determination of the transfer parameters

The energy transfer coefficient, W_{25}, is an important parameter to evaluate the probability of energy transfer. It is well known that

the energy transfer efficiency can be obtained by measuring the fluorescence lifetimes of the $^2F_{5/2}$ level of Yb^{3+} ions [17]

$$\eta = \frac{P}{P + A_{21} + W_{21}^{NR}} = 1 - \frac{\tau}{\tau_0} \tag{9}$$

where P is the energy transfer probability, τ_0 and τ, are the lifetimes of $^2F_{5/2}$ level of Yb^{3+} in the single Yb^{3+}-doped and the Er^{3+} and Yb^{3+} co-doped crystals, respectively. It can be derived from Eq. (1) that

$$P = W_{25}N_3$$

Then we have

$$W_{25} = \frac{\eta \cdot \left(A_{21} + W_{21}^{NR}\right)}{(1-\eta)N_3} \approx \frac{\eta}{(1-\eta)N_{Er}\tau_0} \tag{10}$$

For single Yb^{3+}-doped material, the lifetime of the $^2F_{5/2}$ level is difficult to be obtained accurately because of the radiation trapping [18]. Some authors have introduced a method to obtain the lifetime of the single Yb^{3+}-doped YAB crystal without the influence of radiation trapping and the value is 533 μs [19]. τ in the co-doped materials are 103 μs, 30 μs, and 17 μs, respectively. So the energy transfer efficiencies are 80.7%, 94.4%, 96.8%, respectively. It shows that the energy transfer from Yb^{3+} to Er^{3+} is very efficient. The dependence of transfer efficiency on Yb^{3+} concentration is shown in Fig. 4. The energy transfer efficiency increased with the increasing Yb^{3+} concentration because the energy migration becomes more effective with decreasing donor–acceptor distances. Substituting the value of energy transfer efficiency η into Eq. (10), the energy transfer coefficient W_{25} can be obtained and listed in Table 2.

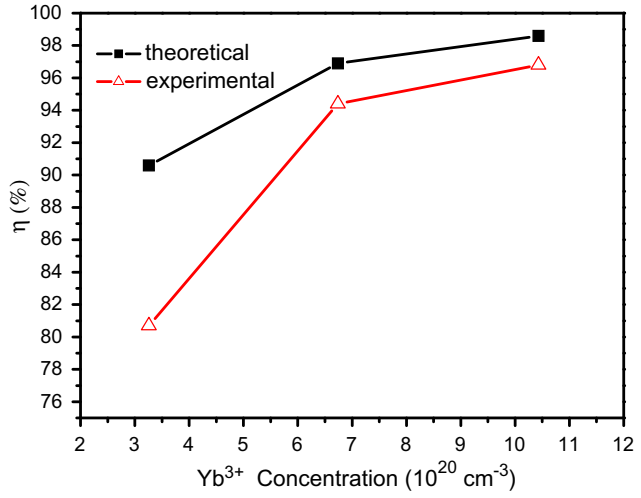

Fig. 4. Comparison of the energy transfer efficiencies obtained from the experiment and theory. The solid lines are guide for the eyes.

The energy transfer efficiency can be also calculated using the critical interaction distance [20]

$$\eta = \frac{R_0^6}{R_0^6 + R^6} \tag{11}$$

where R is the average donor–acceptor distance, which depends on the total Yb^{3+} and Er^{3+} ion concentration N and follows the relation $R = \left(\frac{3}{4\pi N}\right)^{1/3}$ [21]. R_0 is the critical interaction distance, at which the energy transfer efficiency is 50% and can be expressed by [6]

$$R_0^6 = \frac{3c\tau_0}{8\pi^4 n^2} \int \sigma_{em}^{Yb}(\lambda)\sigma_{abs}^{Er}(\lambda)\mathrm{d}\lambda \tag{12}$$

where n is the refractive index of crystal and c is the velocity of light. The calculated critical interaction distance is listed in Table 2. According to Eq. (11), the energy transfer efficiencies for #1, #2 and #3 samples are 90.6%, 96.9% and 98.6%, respectively. The comparison of the energy transfer efficiencies calculated by Eq. (9) (experimental) and Eq. (11) (theoretical) is shown in Fig. 4. It can be seen from the figure that in the high Yb^{3+} concentration (>10 at.%), the energy transfer efficiencies calculated by experiment are accordant with those calculated by theory. But in the low Yb^{3+} concentration (<10 at.%), the value calculated by experiment is discordant with that calculated by theory. The discrepancy may be due to the fact that in the low Yb^{3+} concentration, not all the Yb^{3+} ions are near to the Er^{3+} ions, some energies can not be transferred to the Er^{3+} ions, so the energy transfer efficiency calculated by experiment is lower than that calculated by theory.

In addition, the micro-parameters of energy transfer C_{DA} and energy migration C_{DD} are important parameters for energy transfer. These two parameters corresponding to the Yb^{3+}–Er^{3+} interaction and Yb^{3+}–Yb^{3+} interaction can be derived from Dexter [22]

$$C_{DA} = \frac{3\hbar^4 c^4 Q_A A_D}{4\pi n^4} \int \frac{F_A(E) f_D(E)}{E_4}\mathrm{d}E$$
$$C_{DD} = \frac{3\hbar^4 c^4 Q_D A_D}{4\pi n^4} \int \frac{F_D(E) f_D(E)}{E_4}\mathrm{d}E \tag{13}$$

where $\hbar = h/2\pi$, h is plank constant. $Q_{A(D)} = \int \sigma_{abs}(E)\mathrm{d}E$ is the integral absorption cross-section σ_{abs} of acceptor Er^{3+} (donor Yb^{3+}) transition within 900–1100 nm. $F_{A(D)}$ and $f_D(E)$ are the normalized absorption and emission cross-section line shape of Er^{3+} (Yb^{3+}) and Yb^{3+} ion, respectively. $A_D = A_{21}$ is the radiative transition probabilities between $^2F_{5/2}$ and $^2F_{7/2}$ level of Yb^{3+} ion and can be calculated by the following equation [23]:

$$A_D = A_{21} = \frac{1}{\tau_r} \tag{14}$$

$$\tau_r = \frac{\bar{\lambda}^4}{8\pi c n^2 \int \sigma_{em}(\lambda)\mathrm{d}\lambda} \tag{15}$$

$$\bar{\lambda}^4 = \int \lambda^4 g(\lambda)\mathrm{d}\lambda \tag{16}$$

Table 2
Comparison of energy transfer parameters in some Yb^{3+} and Er^{3+} co-doped crystals

Sample	YLF	YCOB	YAB		
			#1	#2	#3
Yb^{3+} concentration (10^{20} ions/cm^3)	14.0	8.8	3.26	6.74	10.43
Er^{3+} concentration (10^{20} ions/cm^3)	1.4	0.88	0.92	0.83	0.81
C_{DA} (10^{-39} cm^6 s^{-1})	4.1	2.69		5.1	
C_{DD} (10^{-39} cm^6 s^{-1})	19.0	8.45		28.8	
Yb–Er critical interaction distance R_0 (Å)	16	7.7		12.1	
Transfer coefficient W_{25} (10^{-16} cm^3 s^{-1})	0.021	1.3	0.87[a]	3.90[a]	6.84[a]
			1.36[b]	2.82[b]	4.37[b]
Reference	[20]	[21]		This work	

[a] Calculated by Eq. (10).
[b] Calculated by Eq. (17).

where τ_r is the radiative lifetime of $^2F_{5/2}$ level of Yb^{3+}, $\sigma_{em}(\lambda)$ is the emission cross-section at the wavelength λ, and the $g(\lambda)$ is the normalized line shape function All the quantities contributing to the micro-parameters C_{DA} and C_{DD} can be also determined experimentally. In our calculation, $A_D = 1590\ s^{-1}$ and we obtained

$$C_{DA} = 5.1 \times 10^{-39}\ cm^6\ s^{-1}$$

This value is comparable with those determined in other Yb^{3+} and Er^{3+} co-doped materials, such as $4.1 \times 10^{-39}\ cm^6\ s^{-1}$ for Yb, Er:YLF crystal [24] and $2.69 \times 10^{-39}\ cm^6\ s^{-1}$ for Yb, Er:YCOB crystal [25].

Similarly, the energy migration micro-parameter between Yb^{3+} ions can be calculated

$$C_{DD} = 2.88 \times 10^{-38}\ cm^6\ s^{-1}$$

On the other hand, Tkachuk [26] introduced another method to calculate the energy transfer coefficients (W_{25}) according to the C_{DA} and C_{DD}

$$W_{25} = \frac{4\pi^3\sqrt{2\pi}}{9} N_{Yb} \sqrt{C_{DA} C_{DD}} \quad (17)$$

The values of W_{25} calculated by Eq. (17) with different Yb^{3+} concentrations are also summarized in Table 2 and compared with those calculated by Eq. (10). It can be seen from the table that the W_{25} calculated by Eq. (17) are accordant with those calculated by Eq. (10) and in YAB crystal, the energy transfer coefficients are comparable with or higher than those in other materials, which means that the energy transfer from Yb^{3+} to Er^{3+} can be more efficient.

4. Conclusion

The Yb^{3+} to Er^{3+} energy transfer in YAB crystal have been investigated in this paper. The energy transfer coefficients (W_{25}) have been determined by using the simplified rate equations and compared with those calculated by Tkachuk model. In the Yb, Er:YAB crystal, the energy back transfer is not considered because of the high phonon energy of borates, causing almost all the $^4I_{11/2}$ population rapidly non-radiative transition to $^4I_{13/2}$ level of Er^{3+} ions. The other parameters, such as micro-parameters of energy transfer and energy migration and the transfer efficiencies are also determined. The transfer efficiencies are very high. The results show that the energy transfer from Yb^{3+} to Er^{3+} ions is very efficient. So the Yb^{3+} and Er^{3+} co-doped YAB crystal may be a good candidate for the 1.55 μm laser media.

References

[1] K. Kopczynski, Z. Mierczyk, S.M. Kaczmarek, SPIE 3186 (1997) 292.
[2] W.J. Miniscalco, J. Lightwave Technol. 9 (1991) 234.
[3] L.D. da Vila, L. Gomes, L.V.G. Tarelho, S.J.L. Ribeiro, Y. Messadeq, J. Appl. Phys. 93 (2003) 3873.
[4] E. Cantelar, J.A. Munoz, J.A. Sanz-Garcia, F. Cusso, J. Phys.: Condens. Mat. 10 (1998) 8893.
[5] B. Denker, B. Galagan, L. Ivleva, V. Osiko, S. Sverchkov, I. Voronina, J.E. Hellstrom, G. Karlsson, F. Laurell, Appl. Phys. B 79 (2004) 577.
[6] J.F. Philipps, T. Topfer, H. Ebendorff-Heidepriem, D. Ehrt, R. Sauerbrey, Appl. Phys. B 72 (2001) 399.
[7] T. Omatsu, Y. Kato, M. Shimosegawa, A. Hasegawa, I. Ogura, Opt. Commun. 118 (1995) 302.
[8] N.I. Leonyuk, L.I. Leonyuk, Prog. Cryst. Growth Charact. Mater. 31 (1995) 179.
[9] A. Brenier, J. Lumin. 92 (2001) 199.
[10] P. Dekker, J.M. Dawes, J.A. Piper, Y. Liu, J. Wang, Opt. Commun. 195 (2001) 431.
[11] N.A. Tolstik, S.V. Kurilchik, V.E. Kisel, N.V. Kuleshov, V.V. Maltsev, O.V. Pilipenko, E.V. Koporulina, N.I. Leonyuk, Opt. Lett. 32 (2007) 3233.
[12] Y. Chen, Y. Lin, X. Gong, Q. Tan, Z. Luo, Y. Huang, Appl. Phys. Lett. 89 (2006) 241111.
[13] W. You, Y. Lin, Y. Chen, Z. Luo, Y. Huang, J. Cryst. Growth 270 (2004) 481.
[14] D.E. McCumber, Phys. Rev. 136 (1964) A954.
[15] P. Wang, J.M. Dawes, P. Dekker, D.S. Knowles, J.A. Piper, J. Opt. Soc. Am. B 16 (1999) 63.
[16] I. Foldvari, E. Beregi, A. Munoz F, R. Sosa, V. Horvath, Opt. Mater. 19 (2002) 241.
[17] R. Reisfeld, Struct. Bond. 30 (1976) 65.
[18] D.S. Sumida, T.Y. Fan, Opt. Lett. 19 (1994) 1343.
[19] J. Liao, Y. Lin, Y. Chen, Z. Luo, E. Ma, X. Gong, Q. Tan, Y. Huang, J. Opt. Soc. Am. B 23 (2006) 2572.
[20] T. Forster, Discuss. Faraday. Soc. 27 (1959) 7.
[21] D.F. de Sousa, J.A. Sampaio, L.A.O. Nunes, M.L. Baesso, A.C. Bento, L.C.M. Miranda, Phys. Rev. B 62 (2000) 3176.
[22] D.L. Dexter, J. Chem. Phys. 21 (1953) 836.
[23] Y. Chen, X. Lin, Y. Lin, Z. Luo, Y. Huang, Solid State Commun. 132 (2004) 533.
[24] C. Wyss, W. Luth, H.P. Weber, P. Rogin, J. Hulliger, Opt. Commun. 144 (1997) 31.
[25] P.A. Burns, J.M. Dawes, P. Dekker, J.A. Piper, H. Jiang, J. Wang, IEEE J. Quantum Electron. 40 (2004) 1575.
[26] A.M. Tkachuk, S.I. Klokishner, Opt. Spectrosc. 61 (1985) 55.